

Interdependencies in Electrode Manufacturing: A Comprehensive Study Based on Design Augmentation and Explainable Machine Learning

Sajedeh Haghi⁺,*^[a] Yao Chen⁺,^[a] Annika Molzberger⁺,^[a] and Rüdiger Daub^{+[a]}

Electrode manufacturing, as the core of battery cell production, is a complex process chain with a large number of interrelated parameters. An in-depth understanding of the processes, their relevant parameters, and the resulting effects on intermediate and final product properties can accelerate the transition toward quality-oriented, efficient battery cell production. Given the complexity of the process chain, data-driven models have emerged as promising solutions for analyzing the existing interdependencies. The accuracy and effectiveness of these models significantly depend on the quality and comprehensiveness of the underlying data. With a low-quality dataset, there is an increased risk of drawing inaccurate conclusions or generat-

ing misleading results. This article aimed to demonstrate a use case for the evaluation and enhancement of historical datasets to provide a statistically robust foundation for the development of machine learning models. The study was based on pilot-scale anode manufacturing and covered variations in the coating, drying, and calendering processes. The key intermediate product and process parameters were used to predict two primary target variables: adhesion strength and discharge capacity at different C-rates. To gain a better understanding of the analyzed interdependencies, explainable machine learning methods were adopted.

Introduction

The battery system, particularly lithium-ion battery (LIB), is one of the promising technologies for the transition toward a net-zero future. Although alternative solutions such as solid-state, sodium-ion, or lithium-sulfur batteries have been developed over the recent years, LIBs are anticipated to dominate the market in the coming years.^[1] While significant advancements have been achieved over the last decade in both material and production domains, the manufacturing of LIBs still holds potential for improvement,^[2] particularly in terms of cost and throughput.^[1]

The production process of LIB comprises a lengthy chain of interrelated processes. The multitude of process parameters, coupled with limited insight into their collective impact on both intermediate and final product properties, along with high material costs, results in a cost-intensive scrap in battery production.^[2] The electrochemical properties of the batteries, which play a key role in their performance, are primarily established during electrode manufacturing.^[3] Hence, an in-depth and comprehensive understanding of electrode manufacturing is

essential. Through the comprehension of the complexities within this production phase, a foundation for quality-oriented and efficient battery cell production can be established.

Over recent years, data-driven methods have become more prominent in the analysis of the LIB cell production chain,^[4–8] with several studies focusing on electrode manufacturing.^[9–14] In a comprehensive mapping study, HAGHI ET AL.^[15] provided an overview of the existing machine learning (ML) studies, including the analyzed processes, parameters, and adopted algorithms, and highlighted the areas that have been less explored. Most of the existing studies concentrate on single process steps. This focus can hinder a holistic analysis encompassing the entire electrode manufacturing, thereby limiting a complete understanding of the interconnected steps and their cumulative effects.^[15] While the coating process was identified as one of the most analyzed processes in the data-driven studies, the drying process, particularly on the pilot scale, received limited attention.^[15] Additionally, a set of overarching topics have been identified that need to be addressed to accelerate the use of ML in battery cell production. These include thorough documentation of the model development steps, containing data collection, description, and evaluation, as well as incorporation of eXplainable Machine Learning (eXML) methods to increase interpretability and transparency. FARAJI NIRI ET AL.^[16] have reviewed the application of XML methods in the battery value chain, from cell production to state and performance estimation. Their review also includes the fundamentals concerning different XML methods. While ML has received significant attention over the last five years in the battery community, the potential of innovative XML methods remains largely untapped, particularly within the battery cell production field.^[16]

[a] S. Haghi,⁺ Y. Chen,⁺ A. Molzberger,⁺ Prof. Dr. R. Daub⁺
Institute for Machine Tools and Industrial Management
Technical University of Munich
Boltzmannstr. 15, Garching 85748 (Germany)
E-mail: sajedeh.haghi@iwb.tum.de

^{††} All authors have read and agreed to the published version of the manuscript.
 Supporting information for this article is available on the WWW under
<https://doi.org/10.1002/batt.202300556>

 © 2024 The Authors. Batteries & Supercaps published by Wiley-VCH GmbH.
This is an open access article under the terms of the Creative Commons Attribution License, which permits use, distribution and reproduction in any medium, provided the original work is properly cited.

In the previous publication presented by HAGHI ET AL.,^[17] an effort was made to address some of the outlined gaps. The study aimed for an effective analysis of interdependencies between the coating, drying, and calendering processes. To achieve this, the Design of Experiments (DoE) method was employed for data generation. The analysis was based on the mass loading, the temperature of the second dryer, and the porosity as the main influential parameters. The XML methods were adopted to understand the impact of the analyzed parameters on a set of target variables. The results indicated that the temperature of the second dryer, particularly at lower mass loadings, had a negligible impact on both the adhesion and the rate capability of the battery.^[17] A plausible rationale for this observation was based on the primary stages of the drying process, and the assumption that, within the analyzed ranges, the phase critical to the electrode quality predominantly occurred in the first dryer. To provide further clarity, a brief overview of the key stages of the drying process is presented below.

The drying process can be broken down into three main phases. Film shrinkage is the initial phase in which the thickness of the wet film is reduced, resulting in a more compact and consolidated wet film. Pore emptying is the second and often recognized as the most critical phase, especially when discussing drying rates and the subsequent electrode quality. During this phase, the pores of the film are progressively emptied, a process that is driven by capillary forces. An excessive drying rate during this stage can cause binders to migrate to the surface of the film, resulting in compromised structural integrity and a reduced adhesion strength. The final phase of the drying process is centered around the evaporation of any remaining liquid clusters in the film.^[18,19] Identifying the specific time window and the dryer at which the film shrinkage phase ends can be extremely beneficial, as it allows for optimal conditions during the pore emptying stage, leading to a more efficient drying process and improved electrode quality.^[20]

Building upon the findings of the previous study and the formulated assumption,^[17] this article aims to present a comprehensive analysis by incorporating additional parameters involved in the drying process, specifically the temperature of the first dryer and the drying web speed. In this work, a systematic methodology is presented, emphasizing the critical evaluation of historical data, especially in the context of data consolidation. Furthermore, the study demonstrates the capabilities of design augmentation in improving data quality. Based on the improved and extensive dataset, supervised ML models, specifically Support Vector machine (SVM) and Random Forest (RF) were developed, and XML methods were employed to delve into the complexities embedded within these models. The combination of data evaluation with design augmentation and XML methods ensures not only robust modeling but also a clear understanding of the inherent complexities.

The remaining of this article is organized as follows. The next section highlights the relevance of historical data and data quality, and describes possible methods for evaluation and enhancement of dataset. Subsequently, a brief overview of the relevant aspects related to the model development is presented, followed by a discussion of the findings concerning mechanical

and electrochemical properties as target variables. The last section wraps up with concluding remarks and provides a perspective on further research activities.

Design Augmentation to Enhance the Historical Dataset

The majority of the existing studies showcase the potential of ML application in battery cell production based on data obtained from individual targeted analysis. However, it should be noted that in a digitalized production, data collection is an ongoing and iterative process. Continuous collection of data results in a richer dataset that can be used as the foundation for a holistic in-depth analysis of various aspects of production. Figure 1 illustrates a modified version of the Cross-Industry Standard Process for Data Mining (CRISP-DM),^[21] tailored to the requirements and challenges of ML projects.^[22] In today's rapidly changing environments, with various sources of data and real-time streams available, the data collection is recognized as a continuous phase, integrating a more dynamic project flow compared to the conventional CRISP-DM approach. Based on the initial run of model development, the insights derived can prompt the acquisition of further data or the exploration of new aspects. This dynamic perspective underscores that data collection is not a one-time activity. Instead, in an ML project, there is a continuous adaptation, often driven by insights from the modeling and the evaluation steps.

Additionally, the modified framework highlights the importance of monitoring and maintaining deployed data-driven models. This necessity originates from various factors such as data drift, changes in data distribution, or issues related to latency and computational efficiency.^[23] These factors can adversely impact the model's performance. Therefore, regular oversight and timely updates of the models are indispensable to ensure their reliability, accuracy, and effectiveness in real-world applications.

When consolidating historical data, the data quality and its attributes are crucial aspects to investigate, prior to model

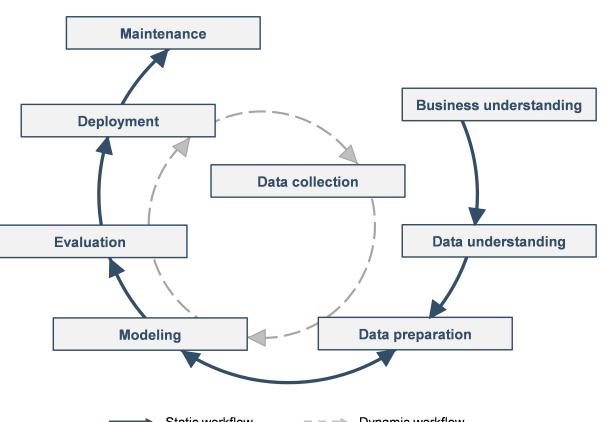


Figure 1. Modified CRISP-DM for ML projects, adapted from Ref. [22], reproduced with permission.

development. Frequently, historical data, especially when generated on a pilot line, stems from a collection of studies, each designed with distinct objectives and analyzed within a certain context. As a result, there is a possibility of encountering biases or discrepancies that can significantly influence the modeling and the subsequent results. Consolidating such data goes beyond mere aggregation; it requires a thorough understanding and evaluation of the dataset. When appropriate, adjustments or enhancements may be essential to guarantee the data's reliability and relevance for model development. The importance of data quality, often encapsulated by the "garbage in, garbage out" principle, is well-recognized in data-driven studies.^[24] This article presents a use case for the thorough evaluation and enhancement of a dataset, aiming for a comprehensive analysis of interdependencies in electrode manufacturing, enabled by ML and XML methods.

There are various statistical methods that can be employed to evaluate the data and its predictive capability.^[25] In this article, the Pearson correlation matrix, the Variance Inflation Factor (VIF), and the Fraction of Design Space (FDS) are used. The results are discussed in the following.

The historical data adopted as the foundation of this study was generated on the pilot production line of the Institute for Machine Tools and Industrial Management at the Technical University of Munich. This includes a roll-to-roll coating machine equipped with three infrared dryers. The details concerning the experimental setup, machinery, and materials align with those documented in Ref. [17] and are available in the supplementary materials.

In the previous study,^[17] the impact of mass loading and porosity in combination with the drying temperature of the second dryer was analyzed. This article aims to broaden the experimental scope by consolidating historical data, consisting of varying parameters in the drying process. The historical data consists of two datasets: the first one is based on the data published in Ref. [17] while the other one includes variations in mass loading, porosity, and the temperature of the first dryer. Within each dataset, the rest of the drying conditions—drying web speed and temperature of the other two dryers—remain consistent. However, these conditions differ between the two datasets. For instance, the drying web speed in the first dataset was set to 0.6 m/min, while the electrodes generated in the second dataset were dried at 0.7 m/min. These variations should enable a detailed analysis of the impact of diverse parameters, including the temperatures of the first and second dryers and drying web speed. Before proceeding to model development, the data quality is evaluated to ensure its statistical robustness and suitability for subsequent analysis.

Figure 2 presents the correlation matrix based on the historical data for potential input parameters for model development. From the correlation matrix, it is evident that there is a strong correlation between drying web speed and the temperature of the first dryer. This correlation indicates the limitations of the existing dataset for an independent analysis of these parameters. A potential solution to handle this issue is design augmentation. Design augmentation involves conducting additional runs to ensure comprehensive coverage of the design

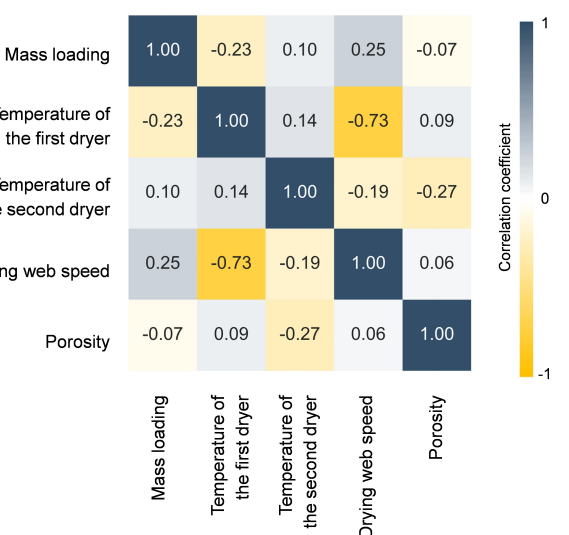


Figure 2. Correlation matrix for the potential input parameters based on the historical dataset.

space, thereby enhancing the data quality.^[25] Through refinement of the dataset, design augmentation enables a more accurate and individual analysis of each parameter's influence.^[25] This refinement is crucial not only to ensure the reliability and validity of the subsequent models developed but also to provide a solid foundation for a thorough examination of the complex interdependencies in electrode manufacturing.

Different methods can be used for design augmentation, all aiming to enhance the design space by improving the resolution or incorporating additional, initially overlooked factors.^[26,27] In this study, the Maximin distance design^[28] was adopted. This method is one of the space-filling designs that aims for optimal coverage of the design space by maximizing the minimum distance between any pair of design points and ensuring a homogenous filling of the design space.^[27] The design augmentation was conducted using Design-Expert® software, taking into account the existing constraints based on domain know-how. Within the analyzed ranges, a practical example of such a constraint is the combination of the highest drying web speed with the lowest drying temperatures and the highest mass loading, resulting in an electrode that is not fully dried at the end of the production line. Table 1 outlines the ranges of the considered factors. For the augmentation, the porosity range was limited to 27–32%.

Table 1. Overview of the considered parameters as factors and their ranges.

Process	Factor	Range
Coating	Mass loading* (mg/cm ²)	8.2–11.2
Drying	Temperature of the first dryer (°C)	45–55
	Temperature of the second dryer (°C)	50–65
	Drying web speed (m/min)	0.6–0.9
Calendering	Porosity (%)	25–40

* Range reported for Active Material (AM).

following the state of the art.^[29] The historical dataset, along with the final one after design augmentation, can be found in the supplementary information.

Figure 3 shows the correlation matrix of the final dataset after design augmentation. With the correlation coefficients below 0.3, all parameters exhibit weak correlation,^[30] making the enhanced dataset suitable for modeling, application of XML methods, and comprehensive analysis of the quality-relevant parameters and the existing interdependencies.

The VIF is another quality indicator that can be used to assess the dataset and identify multicollinearity among the input

variables.^[31] Table 2 provides the VIF values both before and after design augmentation for the analyzed parameters. Considering the complex interrelations among the parameters, the two-factor interactions were additionally included in the design evaluation. The historical data showed a high VIF, surpassing 10, indicating the existence of multicollinearity.^[32] Additionally, the drying web speed and a set of two-factor interactions were identified as aliases, making it unfeasible to delineate their individual impacts on the target variables. Through design augmentation, the VIF values of all terms considered fell within an acceptable range.

The FDS is another valuable technique than can be used to gain insights into the prediction capability of a dataset.^[33] Figure 4 presents the smoothed FDS plots, using the prediction errors, for both historical and augmented data. Based on the modelling techniques adopted in this study (see next Section), the SVM is shown in this example as a representative model to predict the adhesion strength. The results indicate two significant enhancements achieved through design augmentation. Firstly, the range of prediction errors narrowed down. This is an indicator for more precise models. Secondly, as shown in Figure 4 (b), the curve became more leveled across a large section of the design space. This more flattened curve suggests consistent prediction quality across the entirety of the design space.

Given the main phases of the drying process and their impact on quality-relevant parameters, as outlined in the introduction, the temperature of the third dryer was not considered in the DoE and model development. Nevertheless, it is worth noting that the historical dataset contained data points with two distinct temperatures for the third dryer. To ensure a comprehensive and balanced basis for this study and account for potential variables, this aspect was additionally considered during the design augmentation. Figure 5 offers a comprehensive overview of the historical and enhanced dataset generated through design augmentation. Given the high number of factors, this method of visualization was used, adapted from Ref.,^[34,35] to effectively present the experimental space. The final dataset consisted of 40 distinct electrode configurations.

The additional electrode configurations defined through design augmentation were produced and characterized both mechanically and electrochemically. The mechanical characterization was based on the adhesion strength measurement, while

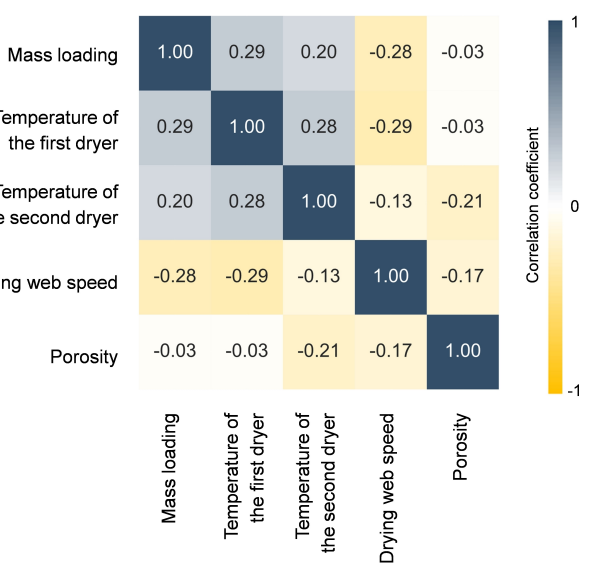


Figure 3. Correlation matrix for the potential input parameters based on the augmented dataset.

Table 2. Comparison of the historical dataset and augmented dataset for main factors and two-factor interactions using VIF.		
Term	VIF	
	Historical dataset	Augmented dataset
Mass loading (A)	33	3
Temperature of the first dryer (B)	4	3
Temperature of the second dryer (C)	1	5
Drying web speed (D)	aliased	5
Porosity (E)	1	10
AB	4	3
AC	1	2
AD	29	3
AE	1	1
BC	aliased	5
BD	aliased	2
BE	2	3
CD	aliased	4
CE	1	2
DE	aliased	10

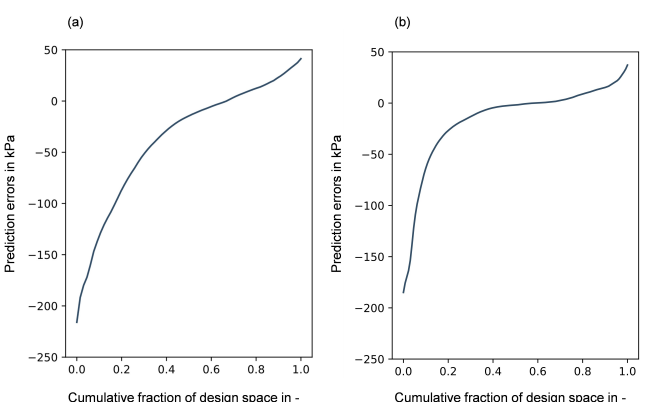


Figure 4. Exemplary FDS plots for prediction of adhesion strength based on (a) historical dataset, (b) augmented dataset.

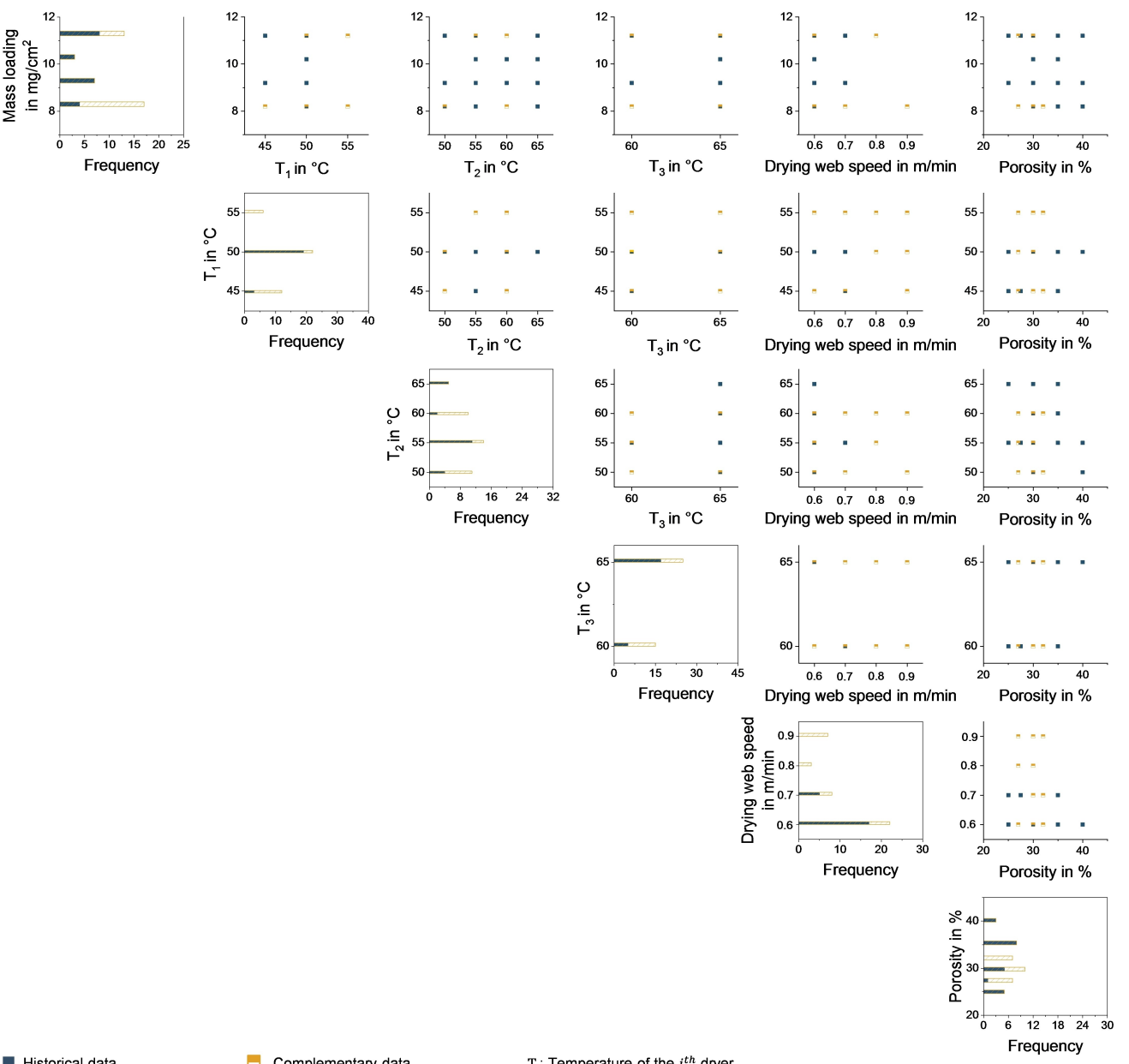


Figure 5. Factor space overview: displaying various factors, their levels and frequencies in the augmented design, including both historical and complementary data points generated through design augmentation.

for the electrochemical characterization full CR2032 coin cells were adopted. The characterizations were carried out on multiple samples, ensuring that the dataset includes at least three data points for each configuration after data cleaning. The detailed information concerning characterization methods and data preparation and preprocessing is available in Ref. [17].

Prediction of Mechanical and Electrochemical Properties Using Data-Driven Models

This section outlines the methods applied for the development of data-driven models using the enhanced dataset, followed by the key findings. In this study, two target variables were chosen. The adhesion, as a crucial mechanical property affecting not only the electrode's processability during the production but also the cell's cyclability and durability,^[36] was defined as a target variable. According to the current state of the art,^[37] this quality-relevant parameter can only be assessed using offline methods. This limitation highlights the necessity of exploring the possibilities to model this target variable using parameters that can be

seamlessly collected inline, ensuring efficient and timely quality control and optimization. The cell rate capability was chosen as the second target variable to investigate the impact of electrode manufacturing parameters on the cell performance.

Approach and Methods

Building upon the findings from the previous study,^[17] sample-specific product parameters such as mass loading and porosity, along with process parameters such as drying temperatures and web speed were used as input parameters for the model development. The models were developed and evaluated using a 5-fold cross-validation approach. Given the size of the dataset, the number of input parameters and the adopted cross-validation approach, RF and SVM were chosen for model development. The performance of the models was evaluated using three metrics: the coefficient of determination, also known as R-squared (R^2), the Root Mean Squared Error (RMSE) and the Mean Absolute Error (MAE). With a range between 0 and 1, a high R^2 indicates a more accurate representation of the data by the model. For RMSE and MAE, lower values are indicative of a better fit to the data, underscoring that the model's predictions are more closely aligned with the actual values.^[38] The reported evaluation metrics were derived from the average values across the folds. Additionally, the standard deviation was calculated, indicating the range of performance across the folds during cross-validation. For the visualization of the model's performance, the parity plot was adopted, with the actual values plotted on the x-axis and the model's predicted values on the y-axis. To prevent the parity plot from becoming too cluttered and ensure a clear overview, only the test data points within each fold were displayed.

To yield deeper insights into the complex interdependencies in electrode manufacturing and transform the so-called *black box* models to *glass box* models,^[39] XML methods were employed. Considering the relatively large number of input features,^[15] the study utilized Accumulated Local Effects (ALE)^[40] and permutation feature importance,^[41] as common XML methods recognized for their robustness and unbiased nature. Additionally, the

SHapley Additive exPlanations (SHAP)^[42] values were used to offer granular, instance-level explanations. The ALE method explores the impact of features on the target variable, and is less sensitive to feature dependencies. The permutation feature importance offers an unbiased assessment of the features by randomly shuffling feature values and observing the consequent changes in model's performance.^[41] While the permutation feature importance method offers insights into the overall relevance of the features and their impact on the target variable, the ALE method visualizes the effect of individual features on the model prediction, factoring in the average effect of the other features. By considering the local effects, ALE plots offer more reliable and unbiased insights into the feature's impact on the model's predictions, compared to global or average effect plots. The SHAP values present both a broad perspective on feature importance and granular insights into individual data points and their impact on the target variable.^[42]

After outlining the relevant details related to model development, the results of the models and XML methods, based on the target variables, are discussed in the subsequent subsections.

Adhesion

Following the data preprocessing, a dataset consisting of 132 data points was used for the model development, predicting the adhesion strength. Figure 6 presents the parity plots for the developed models with the test data points in each fold. These plots provide a visual representation of how well the model predictions align with actual values. Table 3 summarizes the evaluation metrics for the developed models, using a 5-fold cross-validation approach. The RF showed a slightly better performance, compared to SVM with a higher average R^2 value, hence RF was selected for further analysis using XML methods.

Figure 7 reveals the relevance of the input features on the adhesion strength for the developed RF model. Both the permutation feature importance and the SHAP method concur in their findings, with the porosity identified as the most influential parameter impacting the adhesion strength, followed by the mass loading, the temperature of the first dryer, and the drying

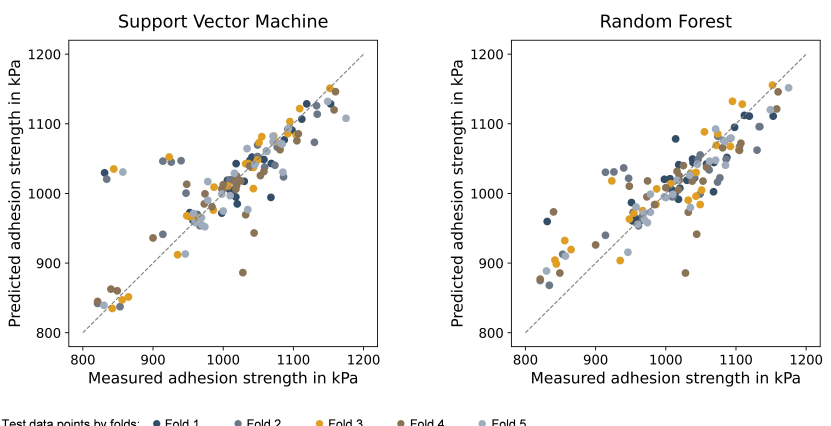


Figure 6. Parity plots of the test data points, with each fold distinguished by color, for the developed models predicting the adhesion strength.

Table 3. Summary of the developed models and the evaluation criteria, calculated using average values across the cross-validation folds, including the standard deviations.

Target Variable	Model	R ²	RMSE	MAE
Adhesion strength	RF	0.72 ± 0.05	42 ± 5	33 ± 4
	SVM	0.65 ± 0.07	47 ± 6	27 ± 5
Discharge capacity after formation	RF	0.99 ± 0.00	0.06 ± 0.01	0.05 ± 0.00
	SVM	0.99 ± 0.00	0.07 ± 0.01	0.05 ± 0.01
Discharge capacity at 0.1 C	RF	0.97 ± 0.01	0.08 ± 0.01	0.06 ± 0.01
	SVM	0.97 ± 0.01	0.09 ± 0.02	0.07 ± 0.02
Discharge capacity at 5 C	RF	0.87 ± 0.03	0.08 ± 0.01	0.07 ± 0.01
	SVM	0.70 ± 0.05	0.13 ± 0.00	0.07 ± 0.02

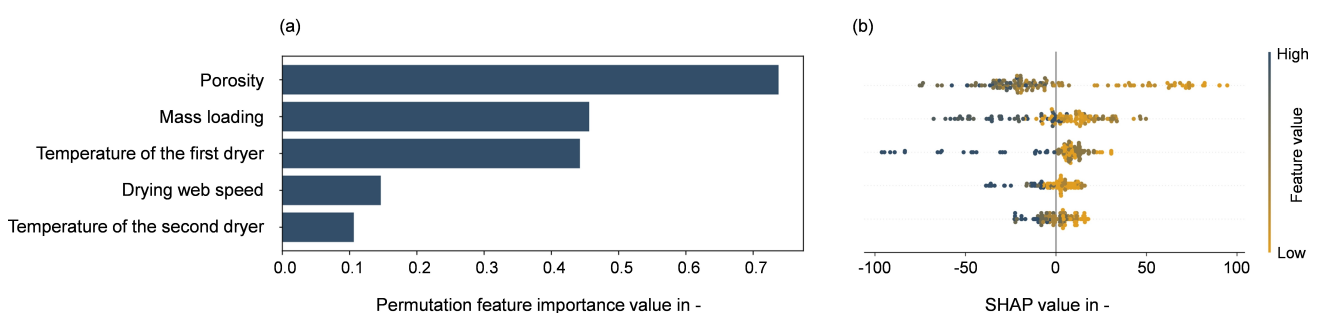


Figure 7. Results of XML methods, revealing the relevance of input features on adhesion as target variable for the developed RF model, using (a) permutation feature importance and (b) SHAP values.

web speed. The temperature of the second dryer was identified as the least relevant parameter within the explored ranges. This finding is consistent with the initial assumption, outlined in the introduction section, which suggested that, given the selected factors and their corresponding levels, the critical phase with the greatest impact on electrode quality during the drying process likely occurred within the first dryer. The bee swarm plot (cf. 7 (b)) reveals additionally the direction in which the parameters impact the adhesion strength. For instance, a low drying web speed results in a higher adhesion strength.

The ALE plots for the influential parameters are presented in Figure 8. For porosity, as shown in Figure 8 (a), it is evident that higher porosity values lead to weak adhesion strength. In the case of mass loading, the same trend was observed, with high mass loading resulting in reduced adhesion strength. The range of ALE values, displayed on the y-axis in each plot, also underscores the magnitude of the feature's impact on the target variable. These observations are in line with the findings presented in Figure 7. It should be noted that the sectional appearance of the ALE plot for continuous values stems from the inherent nature of the RF model, which makes decisions based on tree structures, splitting the data into discrete segments. The drying temperature and speed were considered as discrete features for the ALE analysis. Concerning the temperature of the first dryer, a distinct impact on adhesion strength is observed at 55 °C (cf. 8 (c)). The ALE plot for drying web speed (cf. 8 (d)) reveals that web speed of 0.8 m/min or higher significantly influenced the adhesion strength.

Discharge Capacities

This subsection presents the results of the models developed based on the electrochemical data obtained from the coin cells. A dataset consisting of 123 data points was used for the model development. The discharge capacity after formation was selected as the target variable. Additionally, based on the rate capability test data, the discharge capacity at 0.1 C, hereafter referred to as low C-rate, and 5 C, termed high C-rate, were adopted as target variables.

Figure 9 presents the parity plots for the developed models with the test data points for each fold. Both RF and SVM demonstrated high performance in the prediction of discharge capacity after formation and at low C-rate (see Table 3). This observation aligns with findings from the previous study,^[17] which highlighted that at low C-rates, the discharge capacity is predominantly influenced by the active mass loading, making the prediction task based on the analyzed factors essentially one-dimensional. However, at higher C-rates, the discharge capacity is influenced by a multitude of factors including the porosity and drying conditions. In this case, RF outperformed SVM, with an average R-squared value of 0.87.

To gain a better understanding of the cell's behavior at higher C-rates, XML methods were adopted. Figure 10 presents the results of permutation feature importance and SHAP analysis for the developed RF model. Both methods pinpointed mass loading as the most influential parameter, followed by the porosity and the drying web speed. Among the analyzed parameters, the impacts of the drying temperatures were

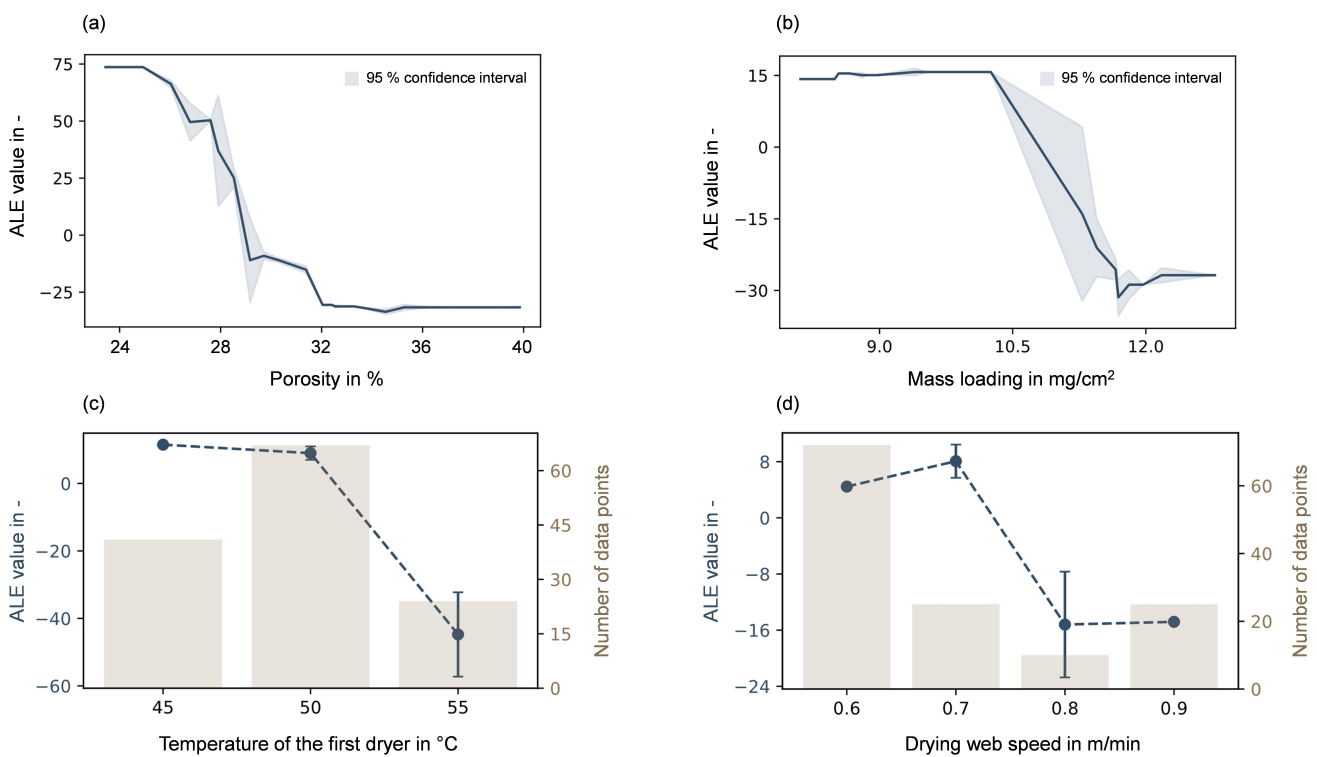


Figure 8. ALE plots illustrating the impact of different features on adhesion strength, with (a) porosity, (b) mass loading as continuous features and (c) temperature of the first dryer and (d) drying web speed as discrete features.

identified as negligible. It should be noted that in the previous study,^[17] the porosity was identified as the most important parameter influencing the discharge capacity at high C-rate, followed by the mass loading. The shifted ranking observed in the current study can stem from the design augmentation being conducted based on a constrained range for porosity. This limitation has likely affected the data distribution and thus the outcomes of the XML methods. Since the range for porosity considered during the augmentation process aligns with industry standards, the findings in this study hold particular significance for practical application within the field.

Figure 11 shows the ALE plots, focusing on the most influential parameters impacting the discharge capacity at a high C-rate and the drying temperature of the second dryer as an example. A high mass loading resulted in a pronounced loss of capacity at a high C-rate (c.f. 11 (a)), which is in line with the findings in the literature.^[43] In the case of the porosity, an inverse trend was observed, with the lowest porosity corresponding to the most significant capacity loss. The drying web speed was identified as the subsequent influential parameter impacting the discharge capacity. As shown in Figure 11 (c), an increase of web speed from 0.6 m/min to 0.7 m/min resulted in a noticeable reduction of discharge capacity. The drying temperature tends to adversely impact the discharge capacity, with a higher temperature leading to a lower discharge capacity at a high C-rate, which is consistent with the findings from the literature.^[44,45] Nevertheless, compared to other analyzed parameters and given the ALE value ranges, the impact appeared to be relatively minor. The results of the developed models and the evaluation metrics

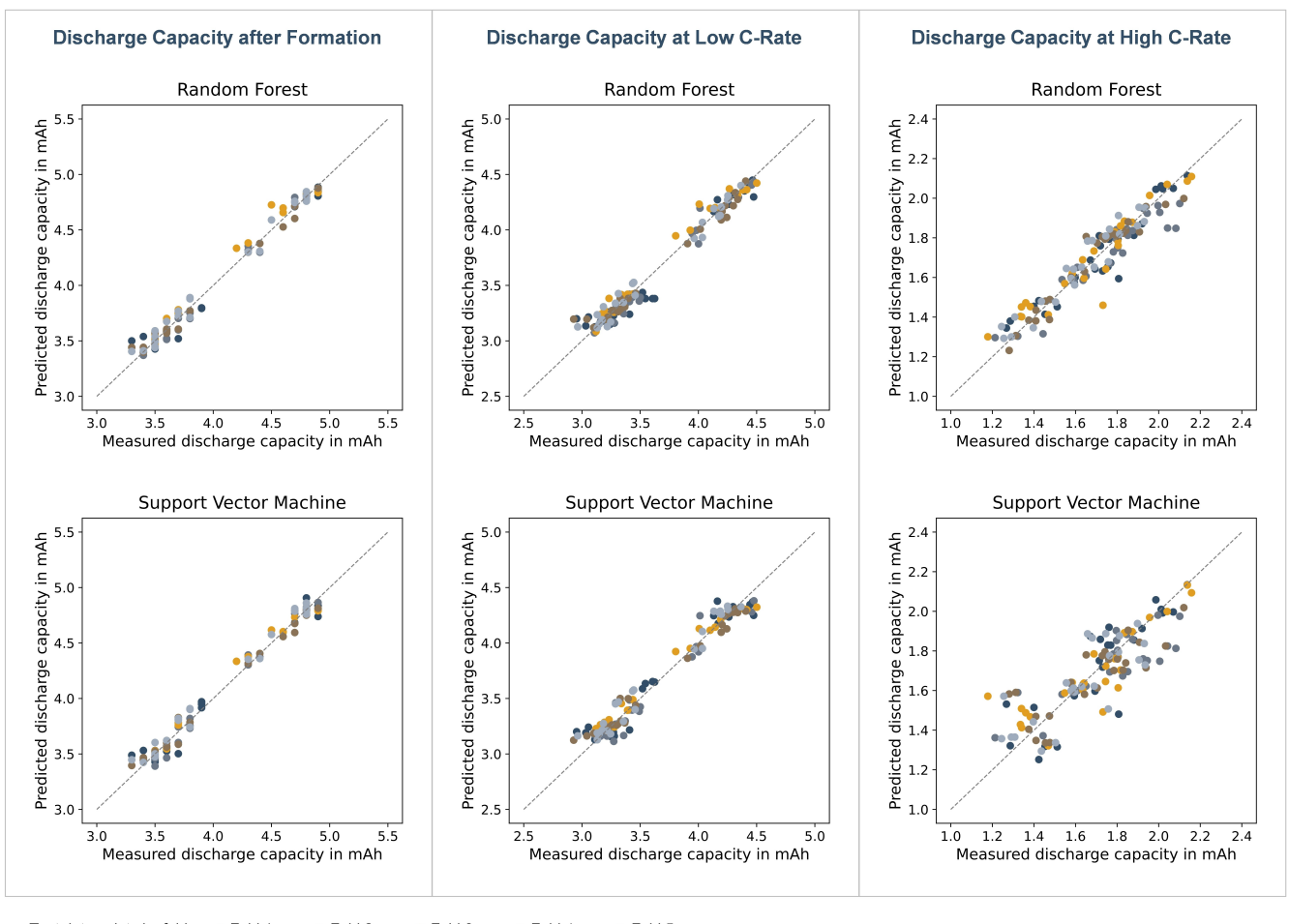
are summarized in Table 3. The details concerning the hyperparameters and the dataset used for the development of the models can be found in the supplementary information.

Conclusions

This article showcased a systematic methodology for consolidation, evaluation and augmentation of historical data, which were used for development of data-driven models. Through design augmentation, a comprehensive dataset consisting of 40 distinct electrode configurations was generated. This enabled a comprehensive analysis of various quality-relevant parameters in the electrode manufacturing of LIB cell, from coating to drying and calendering process. Through an extensive dataset, this article provided the possibility for an exhaustive analysis of the drying process, which so far has received limited attention, particularly on the pilot scale battery production in data-driven literature.^[15]

Adhesion as the mechanical property and cell discharge capacities at different C-rates were adopted as target variables. For model development, RF and SVM were employed alongside a 5-fold cross-validation approach. To gain a better understanding of the underlying decision-making mechanism of the developed models, XML methods were used. Given the relatively large number of features, the permutation feature importance, SHAP, and ALE methods were chosen for the analysis.

In the case of adhesion, porosity emerged as the most influential parameter, with a low porosity, indicating a high compaction rate, leading to improved adhesion strength. Mass



Test data points by folds: ● Fold 1 ● Fold 2 ● Fold 3 ● Fold 4 ● Fold 5

Figure 9. Parity plots of the test data points, with each fold distinguished by color, for the developed models predicting discharge capacity after formation (left), at low C-rate (middle) and at high C-rate (right).

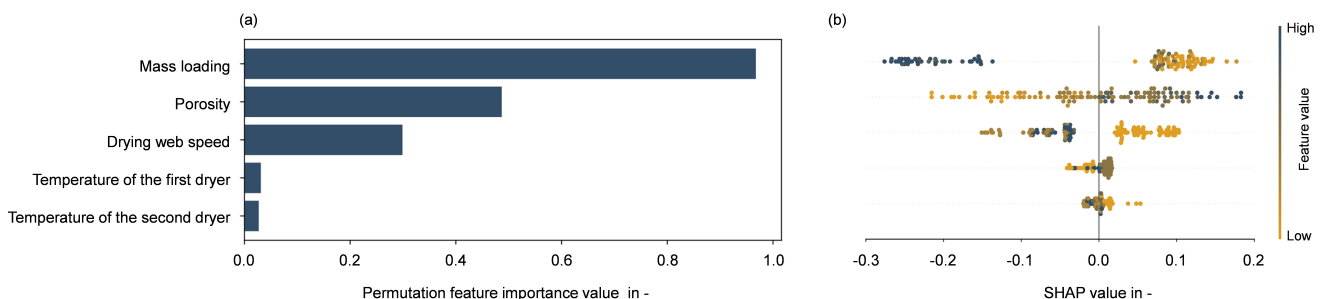


Figure 10. Results of XML methods, revealing the relevance of input features on discharge capacity at high C-rate as target variable for the developed RF model, using (a) permutation feature importance and (b) SHAP values.

loading was the subsequent influential parameter, exhibiting a similar trend. Within the analyzed ranges, the temperature of the first dryer was pinpointed as the third influential parameter, impacting the adhesion strength. This finding is consistent with the hypothesis formulated in the previous study,^[17] which was centered around the occurrence of the pore emptying phase in the first dryer, within the analyzed ranges.

Concerning discharge capacity, both developed models exhibited strong performance at low discharge rates, achieving

an average R^2 value of 0.98. However, at a high C-rate, the RF model demonstrated marginally better performance, with an average R^2 value of 0.87. The results of XML methods quantified the impact of the mass loading, the porosity, and the drying web speed on the discharge capacity at a high C-rate. The drying temperatures were identified as the least influential factors.

This study underscored the relevance of data quality, particularly, when leveraging historical data, and demonstrated how design augmentation can address issues such as high VIF

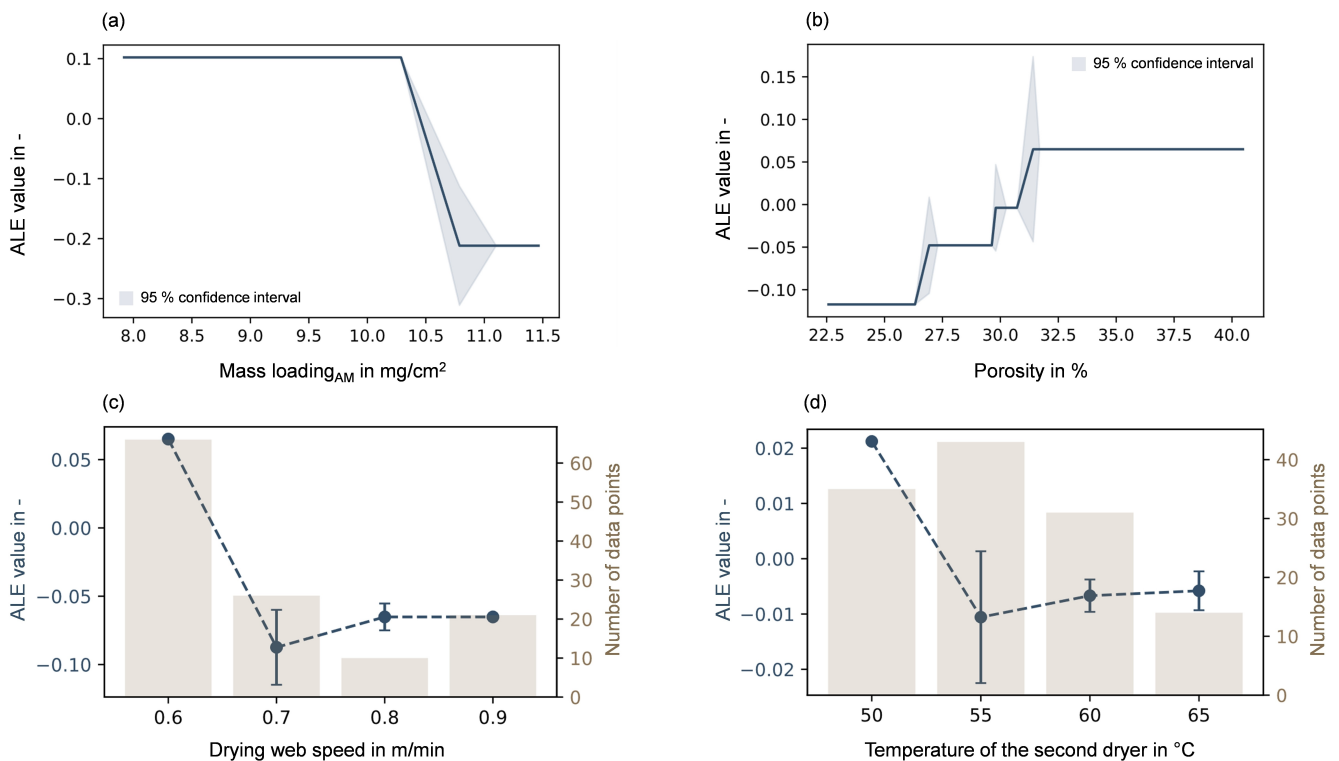


Figure 11. ALE plots illustrating the impact of different features on discharge capacity at high C-rate, with (a) mass loading, (b) porosity as continuous features and (c) drying web speed and (d) temperature of the second dryer as discrete features.

and contribute to the overall quality enhancement of the dataset. To the best of the authors' knowledge, this is the first study in battery cell production that offers a comprehensive overview of potential methods for assessing data quality before developing ML models. An enhanced dataset can facilitate a more refined evaluation of the individual parameters, offering valuable insights into their respective impacts. With five quality-relevant parameters extensively investigated, the findings establish the foundation for in-depth analysis of interdependencies in electrode manufacturing. Given the limited possibilities concerning the inline measurement of adhesion, the developed models can be used as a virtual quality gate, assessing the quality of the intermediate product based on the inline collect parameters. The next possible step is to combine the presented process-specific augmented design with a mixture design, offering the possibility to analyze the impact of slurry's formulation along electrode manufacturing. By offering detailed information on hyperparameters, data preprocessing, and model development, along with providing the dataset comprising 40 distinct electrode configurations, this study can be used as the basis for transfer learning. The developed models can be adopted as starting points and fine-tuned for further analysis based on the data collected from other pilot production lines.

Supporting Information

Supporting information is available online.

Nomenclature

ALE	Accumulated Local Effects
AM	Active Material
CRISP-DM	Cross-Industry Standard Process for Data Mining
DoE	Design of Experiments
FDS	Fraction of Design Space
LIB	Lithium-Ion Battery
ML	Machine Learning
RF	Random Forest
SHAP	SHapley Additive exPlanations
SVM	Support Vector Machine
VIF	Variance Inflation Factor
XML	eXplainable Machine Learning

Author Contributions

Sajedeh Haggi: Conceptualization, Methodology, Investigation, Software, Formal analysis, Data curation, Visualization, Writing - Original Draft. Yao Chen: Data Curation. Annika Molzberger: Investigation, Data Curation. Rüdiger Daub: Funding acquisition, Resources, Supervision, Writing - Review & Editing.

Acknowledgements

This research work was conducted as part of the TrackBatt project (grant number: 03XP0310), funded by the German

Federal Ministry of Education and Research, abbreviated BMBF. The authors gratefully acknowledge the financial support provided by BMBF. The authors would like to thank Josef Keilhofer, Maximilian Lechner, Andreas Mayr, and Filip Dorau for their assistance in electrode manufacturing. The authors also extend their special thanks to Korbinian Heiss, Pengdan He, Wenhua Yao, Hye Min Hong, Nico Schwarz, and Roman Mazur for their support in the characterization of the produced electrodes. Open Access funding enabled and organized by Projekt DEAL.

Conflict of Interests

The authors declare no conflict of interest.

Data Availability Statement

The data that support the findings of this study are available in the supplementary material of this article.

Keywords: design augmentation · historical data · quality · lithium-ion battery · data quality

- [1] Y. Liu, R. Zhang, J. Wang, Y. Wang, *iScience* **2021**, *24*, 102332.
- [2] A. Kwade, W. Haselrieder, R. Leithoff, A. Modlinger, F. Dietrich, K. Droeder, *Nat. Energy* **2018**, *3*.
- [3] T. Günther, N. Billot, J. Schuster, J. Schnell, F. B. Spingler, H. A. Gasteiger, *AM+R* **2016**, *1140*, 304–311.
- [4] A. Turetsky, S. Thiede, M. Thomitzek, N. von Drachenfels, T. Pape, C. Herrmann, *Energy Technol.* **2020**, *8*, 1900136.
- [5] J. Schnell, C. Nentwich, F. Endres, A. Kollenda, F. Distel, T. Knoche, G. Reinhart, *J. Power Sources* **2019**, *413*, 360–366.
- [6] T. Lombardo, M. Duquesnoy, H. El-Bouysidy, F. Åréen, A. Gallo-Bueno, P. B. Jørgensen, A. Bhowmik, A. Demortière, E. Ayerbe, F. Alcaide et al., *Chem. Rev.* **2022**, *122*, 10899–10969.
- [7] M. Duquesnoy, I. Boyano, L. Ganborena, P. Cereijo, E. Ayerbe, A. A. Franco, *Energy and AI* **2021**, *5*, 100090.
- [8] M. Duquesnoy, C. Liu, V. Kumar, E. Ayerbe, A. A. Franco, *J. Power Sources* **2024**, *590*, 233674.
- [9] M. F. Niri, K. Liu, G. Apachitei, L. A. Román-Ramírez, M. Lain, D. Widanage, J. Marco, *Energy and AI* **2022**, *7*, 100129.
- [10] K. Liu, Z. Wei, Z. Yang, K. Li, *J. Cleaner Prod.* **2021**, *289*, 125159.
- [11] S. X. Drakopoulos, A. Gholampour-Shirazi, P. MacDonald, R. C. Parini, C. D. Reynolds, D. L. Burnett, B. Pye, K. B. O'Regan, G. Wang, T. M. Whitehead et al., *Cell Rep. Phys. Sci.* **2021**, *2*, 100683.
- [12] A. C. Ngandjong, T. Lombardo, E. N. Primo, M. Chouchane, A. Shodiev, O. Arcelus, A. A. Franco, *J. Power Sources* **2021**, *485*, 229320.
- [13] E. Rohkohl, M. Schönemann, Y. Bodrov, C. Herrmann, *Adv. Ind. Manuf. Eng.* **2022**, *4*, 100078.
- [14] R. P. Cunha, T. Lombardo, E. N. Primo, A. A. Franco, *Batteries & Supercaps* **2020**, *3*, 60–67.
- [15] S. Haghi, M. F. V. Hidalgo, M. F. Niri, R. Daub, J. Marco, *Batteries & Supercaps* **2023**, *6*, e202300046.
- [16] M. Faraji Niri, K. Aslansefat, S. Haghi, M. Hashemian, R. Daub, J. Marco, *Energies* **2023**, *16*, 6360.
- [17] S. Haghi, J. Keilhofer, N. Schwarz, P. He, R. Daub, *Batteries & Supercaps* **2023**, *e202300457*.
- [18] S. Jaiser, J. Kumberg, J. Klaver, J. L. Urai, W. Schabel, J. Schmatz, P. Scharfer, *J. Power Sources* **2017**, *345*, 97–107.
- [19] J. Kumberg, M. Müller, R. Diehm, S. Spiegel, C. Wachsmann, W. Bauer, P. Scharfer, W. Schabel, *Energy Technol.* **2019**, *7*, 1900722.
- [20] S. Jaiser, A. Friske, M. Baunach, P. Scharfer, W. Schabel, *Drying Technol.* **2017**, *35*, 1266–1275.
- [21] P. Chapman, J. Clinton, R. Kerber, T. Khabaza, T. Reinartz, C. Shearer, R. Wirth, *CRISP-DM 1.0: Step-by-step data mining guide*, **2000**.
- [22] German Mechanical and Plant Engineering Federation (VDMA), *Leitfaden Künstliche Intelligenz - Potenziale und Umsetzungen im Mittelstand (org.) [Artificial Intelligence Guideline - Potentials and Realization in SMEs]*, **2020**.
- [23] E. Ameisen, *Building machine learning powered applications. Going from idea to product*, O'Reilly Media, Sebastopol, CA, **2020**.
- [24] C. Babbage, *Passages from the life of a philosopher*, Dawsons of Pall Mall, London, **1968**.
- [25] W. Kleppmann, *Versuchsplanung - Produkte und Prozesse optimieren (org.) [Design of Experiments - Optimization of Products and Processes]*, Hanser, Munich, **2013**.
- [26] B. J. Nelson, D. C. Montgomery, R. J. Elias, E. Maass, *Qual. Reliab. Eng.* **2000**, *16*, 435–449.
- [27] L. Lu, C. M. Anderson-Cook, *Qual. Reliab. Eng.* **2021**, *37*, 1740–1757.
- [28] M. E. Johnson, L. M. Moore, D. Ylvisaker, *J. Stat. Plan. Inference* **1990**, *26*, 131–148.
- [29] S. Stock, J. Hagemeyer, S. Grabmann, J. Kriegler, J. Keilhofer, M. Ank, J. L. Dickmanns, M. Schreiber, F. Konwitschny, N. Wassiliadis et al., *Electrochim. Acta* **2023**, *471*, 143341.
- [30] B. Ratner, *J. Target Meas Anal Mark* **2009**, *17*, 139–142.
- [31] M. H. Kutner, C. Nachtsheim, J. Neter, W. Li, *Applied linear statistical models*, McGraw-Hill Irwin, Boston, Mass., **2005**.
- [32] K. Siebertz, *Statistische Versuchsplanung (org.) [Design of Experiments (DoE)]*, Springer, Berlin, Heidelberg, **2010**.
- [33] A. Zahran, C. M. Anderson-Cook, R. H. Myers, *JQT* **2003**, *35*, 377–386.
- [34] J. Ma, P. Mahapatra, S. E. Zitney, L. T. Biegler, D. C. Miller, *Comput. Chem. Eng.* **2016**, *94*, 60–74.
- [35] J. C. Eslick, B. Ng, Q. Gao, C. H. Tong, N. V. Sahinidis, D. C. Miller, *Energy Procedia* **2014**, *63*, 1055–1063.
- [36] W. Haselrieder, B. Westphal, H. Bockholt, A. Diener, S. Höft, A. Kwade, *Int. J. Adhes. Adhes.* **2015**, *60*, 1–8.
- [37] S. Haghi, M. Leeb, A. Molzberger, R. Daub, *Energy Technol.* **2023**, *11*, 2300364.
- [38] D. N. Moriasi, J. G. Arnold, M. W. van Liew, R. L. Bingner, R. D. Harmel, T. L. Veith, *Trans. ASABE* **2007**, *50*, 885–900.
- [39] A. Rai, *JAMS* **2020**, *48*, 137–141.
- [40] D. W. Apley, J. Zhu, *J. R. Stat. Soc. Series. B* **2020**, *82*, 1059–1086.
- [41] A. Altmann, L. Tolosí, O. Sander, T. Lengauer, *Bioinformatics* **2010**, *26*, 1340–1347.
- [42] S. M. Lundberg, S.-I. Lee, *Advances in Neural Information Processing Systems* **2017**, *30*, 1–10.
- [43] M. Hidalgo, G. Apachitei, D. Dogaru, M. Faraji-Niri, M. Lain, M. Copley, J. Marco, *J. Power Sources* **2023**, *573*, 233091.
- [44] J. Kumberg, W. Bauer, J. Schmatz, R. Diehm, M. Tönsmann, M. Müller, K. Ly, P. Scharfer, W. Schabel, *Energy Technol.* **2021**, *9*, 2100367.
- [45] S. Jaiser, M. Müller, M. Baunach, W. Bauer, P. Scharfer, W. Schabel, *J. Power Sources* **2016**, *318*, 210–219.

Manuscript received: November 27, 2023

Revised manuscript received: February 26, 2024

Accepted manuscript online: February 26, 2024

Version of record online: March 12, 2024